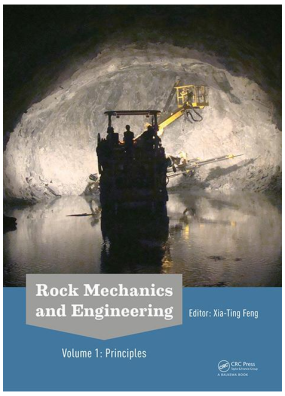

Rock Mechanics and Engineering
Volume I: Principles
Xia-Ting Feng

Practical estimate of rock mass strength and deformation parameters for engineering design

Publication details
https://test.routledgehandbooks.com/doi/10.1201/b20273-19
M. Cai
Published online on: 13 Dec 2016

Chapter 18

Practical estimate of rock mass strength and deformation parameters for engineering design

M. Cai
Bharti School of Engineering, Laurentian University, Sudbury, Ontario, Canada

Abstract: Knowledge of the rock mass strength is required for the design of many engineering structures to be built in or on rocks. For this purpose, it is necessary to obtain design parameters such as deformation moduli, peak and residual strength parameters, and dilation angle for numerical modeling and design. The GSI system, proposed by Hoek *et al.* (1995), is now widely used for the estimation of the rock mass peak strength and the rock mass deformation parameters. A quantitative approach to assist in the use of the GSI system is presented. It employs the in-situ block volume and a joint condition factor as quantitative characterization factors to determine the peak GSI value. To use the GSI system to estimate the residual strength of jointed rock masses, the peak GSI can be adjusted to a residual GSIr value based on the two major controlling factors in the GSI system, *i.e.*, the residual block volume and the residual joint surface condition factor. Methods to estimate peak and residual block volumes and joint surface condition factors are presented. In addition, a detailed discussion on the determination of other design analysis input parameters, such as uniaxial compressive strength of intact rocks and Hoek-Brown constant m_i are given and a method to estimate dilation angles of rock masses is presented.The determined Hoek-Brow rock mass strength parameters, dilation angles, and deformation modulus can be used in numerical analyses for safe and cost-effective engineering design. Because of its quantitative nature, this approach allows the consideration of variability of rock mass strength and deformation parameters in design, using the Monte Carlo or point estimate method.

1 INTRODUCTION

Knowledge of the rock mass strength and deformation behaviors is required for the design of many engineering structures to be built in or on rocks, such as foundations, slopes, tunnels, underground caverns, drifts, and mining stopes. The strength and deformation modulus of a jointed rock mass depends on the strength of the intact rocks and the joint conditions. A better understanding of the mechanical properties of rock masses will facilitate cost-effective design of such structures.

The determination of the global mechanical properties of a jointed rock mass remains one of the most difficult tasks in rock mechanics. Anyone who had practiced in the geomechanics and geotechnical fields will not hesitate to admit that trying to estimate the deformation modulus and uniaxial compressive strength of a jointed rock mass is such a daunting difficult task. There are many reasons why it is so. The name of a rock mass is not CHILE (Continuous, Homogeneous, Isotropic, and Linearly-Elastic) but DIANE (Discontinuous, Inhomogeneous, Anisotropic, and Non-Elastic) (Hudson & Harrison, 1997). Complex spatial variation, scale effect, stress path dependency, and limited access to monitoring and measurement are other factors that render estimating the mechanical properties of a rock mass difficult.

Many researchers have developed constitutive models to describe the strength and deformation behaviors of jointed rock masses (*e.g.*, Oda, 1983; Amadei, 1988; Cai & Horii, 1992). Because there are so many parameters that affect the deformability and strength, it is generally impossible to develop a universal constitutive model that can be used to a priori predict the strength of a rock mass. In addition, model parameters need to be calibrated before the models can be used in design analysis.

Traditional methods to determine the mechanical property parameters include plate-loading tests for deformation moduli and in-situ block shear tests for strength parameters. These tests can only be performed when the exploration adits are excavated and the cost of conducting these tests is high. Although back-analyses, which are based on field measurement, are helpful in determining the strength and deformation parameters as a project proceeds (Cividini *et al.,* 1981; Sakurai & Takeuchi, 1983; Cai *et al.*, 2007), they do not provide design parameters at the pre-feasibility or feasibility study stages.

As computers become much more powerful and high performance computing is now easily accessible, there is a new trend to model the rock mass response using some basic measured mechanical and geometrical properties of the rock and joints as inputs. Jointing is considered using a stochastic discrete fracture network (DFN) simulation (Dershowitz & Einstein, 1988). Many equally significant realizations of the fracture network can be produced. One can pick a particular fracture network realization and then import it into some numerical packages (*e.g.*, ELFEN (Rockfield Software Ltd., 2003), PFC3D (Itasca, 2010)) to create a jointed rock mass model. The approach adopted in PFC3D is called the synthetic rock mass (SRM) approach (Pierce *et al.,* 2007; Mas Ivars *et al.,* 2011). Failure of the rock mass is simulated by considering intact rock fracturing, joint sliding, or the combination of the two. Using this approach, it not only helps us to understand better the failure mechanism of jointed rock masses, but also assists us to estimate rock mass strengths and deformabilities. While the approach is promising, it also bears some major deficiencies. The approach is not simple enough for site engineers to use, and it requires them to be able to run some of the most skill demanding software packages (ELFEN, PFC3D, FRACMAN (Dershowitz *et al.,* 1993)) in the geotechnical community. Computing time is long and there are many model parameters that cannot be directly measured and have to be calibrated using field monitoring data. In addition, the discrete fracture network generated is often a very rough representation of reality (*e.g.*, smooth joint in a large scale, circular or elliptical joint shape etc.), and the limitation of the approach created by the DFN model is often overlooked by some researchers and users.

Some attempts have been made to develop simple methods to characterize jointed rock masses to estimate the deformability and strength indirectly. The Geological Strength Index (GSI), developed by Hoek *et al.* (1995), is one of them. It uses properties of intact rock and conditions of jointing to determine/estimate the rock mass deformability and strength. GSI values can be estimated based on the geological description of the rock mass and this is well suited for rock mass characterization at the initial stage of a project. The GSI system concentrates on the description of two factors, rock structure and block surface conditions. Some efforts (Sonmez & Ulusay, 1999; Russo, 2009; Hoek *et al.,* 2013) were made to make the system more user friendly, but the approach presented in Cai *et al.* (2004), which employs the block volume (V_b) and a joint condition factor (J_c) as quantitative characterization factors, will be presented in this chapter. This approach adds quantitative means to facilitate use of the system, especially by inexperienced engineers. Because of its quantitative nature, it facilitates the use of probabilistic design approach to tunnel and cavern design using the GSI system (Cai & Kaiser, 2006a; Cai, 2011). Furthermore, the approach has been developed and tested for rock mass's residual strength estimation, by adjusting the peak GSI to the residual GSI_r value based on the two major controlling factors in the GSI system – the residual block volume V_b^r and the residual joint condition factor J_c^r (Cai *et al.,* 2007).

Although imperfect, the GSI system provides a simple and yet practical means to define a complete set of mechanical properties (peak and residual Hoek-Brown strength parameters m_b and s, or the equivalent Mohr-Coulomb strength parameters c and ϕ, as well as deformation modulus E) for design purpose.

Firstly some widely used rock mass classification systems and empirical relations to estimate rock mass strength and deformation modulus using these classification systems are reviewed. Next, a complete quantitative approach to determine peak and residual strength parameters of jointed rock masses using the Generalized Hoek-Brown failure criterion and the GSI system is presented. Other input parameters required for engineering design, such as deformation modulus and dilation angle, are also discussed. An example is given to illustrate the application of the proposed method.

2 ROCK MASS CHARACTERIZATION FOR ENGINEERING DESIGN

2.1 Brief summary of rock mass classification systems

Rock mass characterization is the process of collecting and analyzing qualitative and quantitative data that provide indices and descriptive terms of the geometrical and mechanical properties of a rock mass. It is a significant part in any field geological investigation involving rock engineering problems. This process requires the collection and recording as well as analyzing a sizable amount of geological and geotechnical data. Methods for rock mass characterization include core logging, borehole logging, scanline surveying, cell mapping, geologic structure mapping, and rock index testing. New technologies, such as digital image processing of fracture information and laser-based imaging of joint roughness, can be applied for rock mass characterization.

When all necessary data are collected, the rock masses are classified according to the emphasis of influence of certain index on the overall rock mass quality based on a classification system or scheme. Ideally rock mass classification should provide a quick means to estimate the support requirement and to estimate the strength and deformation properties of the rock mass. More specifically, a rock mass classification scheme is intended to classify the rock masses, provide a basis for estimating deformation and strength properties, supply quantitative data for support estimation, and present a platform for communication between exploration, design and construction groups.

Many rock mass classification systems have been proposed and used in engineering practice, such as the Terzaghi's classification (Terzaghi, 1946), RQD (Deere, 1968), RSR (Wickham *et al.,* 1974), RMR (Bieniawski, 1976), Q (Barton *et al.,* 1974; Barton, 2002), GSI (Hoek *et al.,* 1995, 1998), and RMi system (Palmstrøm, 1996a,b). Some systems are based on the modification of the existing ones to suit a specific application. For examples, the RMR system was modified by Laubscher (1990) for mine design and by Kendorski *et al.* (1983) for drift support design in caving mines. The Q system was modified by Potvin (1988) for stope design.

2.2 Estimation of rock mass properties using rock mass classification systems

Rock mass classification systems have been used to estimate mechanical properties (*i.e.*, deformation modulus and uniaxial compressive strength) of jointed rock masses at the preliminary design stage of a project. Table 1 summarizes some of the widely used empirical equations for determining deformation moduli of rock masses from

Table 1 Empirical relations to estimate deformation modulus from a classification index.

No.	*Deformation modulus*	*Reference*	*Note*
1	$E = E_i\,(0.0231RQD\text{-}1.32)$	Coon & Merritt (1970)	RQD>57
2	$E = E_i\,(RQD\text{-}60)/40$	Deer *et al.* (1967)	RQD>60
3	$E = E_i 10^{0.0186\text{RQD}-1.91}$	Zhang & Einstein (2004)	
4	$E = 2RMR-100$	Bieniawski (1978)	Applicable for RMR > 50
5	$E = 0.1(RMR/10)^3$	Read *et al.* (1999)	
6	$E = 10^{\frac{RMR-10}{40}}$	Serafim & Pereira (1983)	Applicable for RMR < 50
7	$E = E_i\left(0.0028RMR^2 + 0.9e^{\frac{RMR}{22.82}}\right)$	Nicholson & Bieniawski (1990)	E_i is the elastic modulus of the intact rock
8	$E = 25\log Q$	Barton *et al.* (1980)	Applicable for Q > 1
9	$E = 10Q_c^{1/3}$, where $Q_c = Q\dfrac{\sigma_c}{100}$	Barton (2002)	σ_c is the strength of intact rock
10	$E = 5.6(RMi)^{0.375}$	Palmstrøm (1995)	For RMi > 0.1
11	$E = \sqrt{\dfrac{\sigma_c}{100}}10^{\frac{GSI-10}{40}}$	Hoek & Brown (1997)	Applicable for σ_c < 100
12	$E = E_i^{(sa)0.4}$, $E_i = 50$ GPa, $s = e^{\frac{GSI-100}{9}}$, $a = 0.5 + \dfrac{1}{6}\left(e^{-GSI/15} - e^{-20/3}\right)$	Sonmez *et al.* (2004)	GSI = RMR

Table 2 Empirical relations to estimate the uniaxial compressive strength of jointed rock masses from a classification index.

No.	*Rock mass to rock strength ratio*	*Reference*	*Note*
1	$\frac{\sigma_{cm}}{\sigma_c} = 10^{0.013RQD-1.34}$	Zhang (2010)	For RQD < 60
2	$\frac{\sigma_{cm}}{\sigma_c} = e^{\left(-0.008J_f\right)}$ $J_f = \frac{J_n}{nr}$	Ramamurthy *et al.* (1985), Ramamurthy (1994)	J_n – number of joints per meter; n – inclination parameter (0.05 to 0.98) depending on the angel between the joint and $\sigma 1$. r – joint strength factor related to joint condition (= tanϕ). For RQD < 60
3	$\frac{\sigma_{cm}}{\sigma_c} = 0.039 + 0.893e^{\left(\frac{-J_f}{160.99}\right)}$	Jade & Sitharam (2003)	For RQD < 60. The definition of J_f is the same as above.
4	$\frac{\sigma_{cm}}{\sigma_c} = e^{7.65\left(\frac{RMR-100}{100}\right)}$	Yudhbir *et al.* (1983)	
5	$\frac{\sigma_{cm}}{\sigma_c} = \frac{MRMR-\text{Rating for } \sigma_c}{106}$	Laubscher (1984)	
6	$\frac{\sigma_{cm}}{\sigma_c} = e^{\left(\frac{RMR-100}{18.75}\right)}$	Ramamurthy *et al.* (1985)	
7	$\frac{\sigma_{cm}}{\sigma_c} = e^{\left(\frac{RMR-100}{20}\right)}$	Sheorey *et al.* (1989)	RMR ≥ 18, 1976 version of RMR.
8	$\frac{\sigma_{cm}}{\sigma_c} = e^{\left(\frac{RMR-100}{24}\right)}$	Kalamaras & Bieniawski (1993)	
9	$\frac{\sigma_{cm}}{\sigma_c} = \frac{RMR}{RMR+6(100-RMR)}$	Aydan & Dalgiç (1998)	
10	$\sigma_{cm} = 7\gamma f_c Q^{1/3}$ MPa	Bhasin & Grimstad (1996)	$f_c = \sigma_c/100$ for Q > 10 and σ_c > 100 MPa, otherwise f_c= 1; and γ is the unit weight of the rock mass in g/cm^3.
11	$\sigma_{cm} = 5\gamma\left(Q\frac{\sigma_c}{100}\right)^{1/3}$ MPa	Barton (2002)	γ is the unit weight of the rock mass in g/cm^3.
12	$\frac{\sigma_{cm}}{\sigma_c} = JP = 0.2\sqrt{jC} \times V_b^{0.37jC^{-0.2}}$	Palmstrøm (1995)	V_b is the block volume and j_c is the joint condition factor

index values such as RQD, RMR, Q, and GSI. Table 2 summarizes some widely used empirical equations for the determination of uniaxial compressive strengths of jointed rock masses.

It is noted that these empirical equations try to link a rock mass classification index value to the deformation modulus and uniaxial compressive strength of a jointed rock mass. They do not provide a complete description of the failure envelopes which are needed in many design analyses. Although GSI appears a few times in the tables, it is fundamentally associated with the generalized Hoek-Brown failure criterion. This failure criterion, since its inception in 1980 (Hoek & Brown, 1980), has undergone a few revisions (Hoek, 1983; Hoek & Brown, 1988; Hoek *et al.,* 1995, 1998, 2002; Hoek & Brown, 1997) and is widely accepted in the engineering community. In the following discussion, we present some extensions and refinements to the GSI system for the estimation of peak and residual strength parameters of jointed rock mass in the context of the generalized Hoek-Brown failure criterion.

3 ESTIMATION OF PEAK AND RESIDUAL STRENGTH PARAMETERS OF JOINTED ROCK MASS USING THE GSI SYSTEM

3.1 Peak strength parameters

3.1.1 Generalized Hoek-Brown failure criterion

The generalized Hoek-Brown failure criterion for jointed rock masses is (Hoek *et al.*, 2002)

$$\sigma_1 = \sigma_3 + \sigma_c \left(m_b \frac{\sigma_3}{\sigma_c} + s \right)^a \tag{1}$$

where m_b, s, and a are constants for the rock mass, and σ_c is the uniaxial compressive strength of the intact rock.To apply the Hoek-Brown failure criterion for estimating the strength of a jointed rock mass, three properties of the rock mass need to be obtained. The first one is the uniaxial compressive strength of the intact rock σ_c, the second is the value of the Hoek-Brown constant m_i for the intact rock, and the last one is the value of GSI for the rock mass. σ_c and m_i can be determined by statistical analysis of the results of a set of triaxial tests on carefully prepared core specimens. The GSI value can be obtained from a chart provided in Hoek *et al.* (1995) or other relevant references. Once the GSI value is known, other Hoek-Brown parameters m_b, s, a are given as (Hoek *et al.*, 2002)

$$m_b = m_i \exp\left(\frac{GSI - 100}{28 - 14D} \right) \tag{2}$$

$$s = \exp\left(\frac{GSI - 100}{9 - 3D} \right) \tag{3}$$

$$a = 0.5 + \frac{1}{6}\left(e^{-GSI/15} - e^{-20/3} \right) \tag{4}$$

where D is a factor between 0 and 1, which depends on the degree of disturbance to which the rock mass has been subjected by blast damage and stress relaxation. For a tunnel excavated by controlled blasting, manual excavation, or Tunnel Boring Machine (TBM) leading to excellent excavation quality, the disturbance to the confined rock mass surrounding the tunnel is minimal and $D = 0$ can be used. When very poor quality blasting in a hard rock tunnel results in severe local damage in the surrounding rock mass, $D = 0.8$. For very poor blasting in rock slopes leading to severe rock mass damage, $D = 1.0$. The D factor can affect the rock mass strength and deformability significantly and sufficient consideration must be given to the selection of this parameter.

3.1.2 Intact rock strength σ_c

Getting σ_c right is the first step toward getting the rock mass properties right. In addition to σ_c, intact rock properties such as tensile strength σ_t, elastic modulus E_i, and Poisson's ratio ν are also needed in design. These parameters can be obtained from laboratory Brazilian test, uniaxial compression test, or triaxial test.

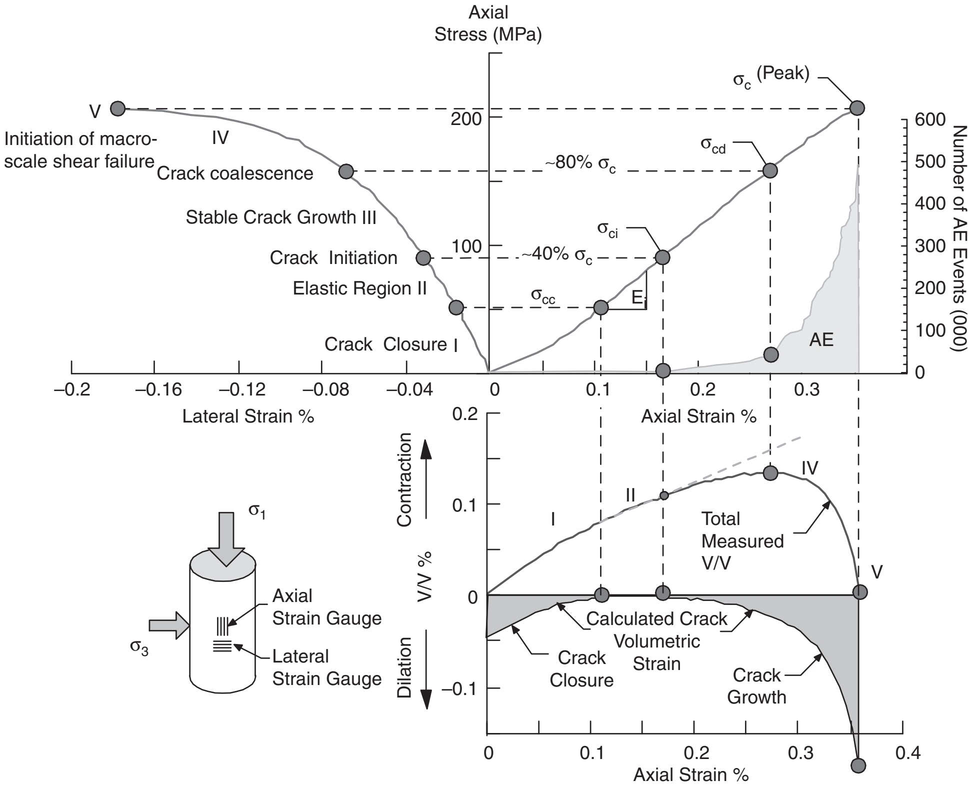

Figure 1 Stress-strain diagram of a rock showing the stages of crack development (Martin, 1993).

A typical stress-strain relations obtained from a uniaxial compression test is presented in Figure 1, where σ_{cc} is the crack closure stress, σ_{ci} is the crack initiation stress, σ_{cd} is the crack damage stress, and σ_c is the peak stress at failure. The three stress thresholds, *i.e.*, σ_{ci}, σ_{cd}, and σ_c, represent important stages in the development of the macroscopic failure process of intact rocks.

In laboratory tests on intact rocks, the crack initiation stress is defined by the onset of stable crack growth or dilatancy, which can be identified from the stress – volumetric strain curve as the point of the departure of the volumetric strain observed at a given mean stress from that observed in hydrostatic loading to the corresponding pressure. Whenever possible, the value of σ_c should be determined by laboratory testing on cores of approximately 50 mm in diameter and 100 mm in length.

One important aspect in obtaining intact rock properties from laboratory tests is sample damage. This is particularly true for engineering design at depth because core samples taken from deep highly stressed ground are very much prone to sample damage, due to stress relaxation. Intact rock strength properties obtained using cores obtained from deep or high stress zones can underestimate the intact rock strength in-situ.

3.1.3 Practical estimate of m_i value

As seen in Equation 2, m_i is a Hoek-Brown model parameter for the intact rock, which can be obtained from triaxial test results (σ_c can also be obtained from triaxial test results). The triaxial test data can be processed using a program called RocData, available from Rocscience Inc.

When time or budget constraints do not allow a triaxial testing program to be carried out, m_i values can be estimated from some tables given in Hoek *et al.* (1995) and Hoek (2007). In the table given by Hoek (2007), possible m_i data ranges are shown by a variation range value immediately following the suggested m_i value. m_i values range from 4 to 33 for some commonly encountered rocks and an impression that m_i depends only on rock type can be seen from the table but this is not true. Rock type cannot be used directly to define the m_i value. The m_i value depends on many factors such as mineral content, foliation, and grain size (texture). There is a large variation range of m_i values and it presents a major challenge for engineers to choose a reasonably accurate m_i value for a particular rock.

Recently, a simple but yet practical method to estimate tensile strength and m_i values of brittle rocks was proposed by Cai (2010). According to the method, the tensile strength σ_t is equal to $\sigma_{ci}/8$; the m_i value is equal to $m_i = 8\ \sigma_c/\sigma_{ci}$ in low confinement zone, where σ_{ci} is the crack initiation stress which can be obtained from the uniaxial compression test, using either volumetric strain measurement or acoustic emission monitoring techniques (see Figure 1). It is found that $m_i = 12\ \sigma_c/\sigma_{ci}$ can be applied to strong, brittle rocks, applicable to high confinement zone. Because rock mass failure around excavation boundaries is governed by low confinement conditions, $m_i = 8\ \sigma_c/\sigma_{ci}$ is recommended for the estimation of m_i values.

m_i values inferred from the literature can only be used when there are no test data available at the initial design stage of a project. Whenever possible, simple laboratory uniaxial compression tests should be conducted to determine σ_{ci},σ_c, and hence m_i values more accurately.

3.1.4 Quantitative determination of GSI value

Having σ_c and m_i values determined, we need to define the GSI value in order to use the generalized Hoek-Brown failure criterion for jointed rock masses. As discussed above, the GSI system has been developed and evolved over many years based on practical experience and field observations. The GSI value is estimated based on geological descriptions of the rock mass involving two factors, rock structure or block size and joint or block surface conditions (Hoek & Brown, 1997). Although careful consideration has been given to the precise wording for each category and to the relative weights assigned to each combination of structural and surface conditions, the use of the original GSI table/chart involves some subjectivity and long-term experiences and sound judgment are required to use the GSI system successfully.

A means to quantify the GSI chart by use of field measurement data, which employs the block volume V_b and a joint surface condition factor J_c as quantitative characterization factors, is presented by Cai *et al.* (2004). The resulting approach adds quantitative measures in an attempt to render the system more objective. By adding measurable quantitative input for quantitative output, the system becomes less dependent on experience while maintaining its overall simplicity. The block volume can be calculated from joint spacings of joint sets. The effect of joint persistence on the block volume can be considered using a joint persistence factor. The joint surface condition factor is obtained by rating joint roughness depending on the large-scale waviness, small-scale smoothness of joints, and joint alteration depending on the weathering and infillings in joints. The quantitative approach was validated using field test data and applied to the estimation of the rock mass properties at some project sites (Alejano *et al.,* 2009; Fischer *et al.,* 2010; Hashemi *et al.,* 2010; Gischig *et al.,* 2011; Ghafoori *et al.,* 2011; Soleiman Dehkordi *et al.,* 2013). This approach adds quantitative means to assist in the selection of modeling parameters and is of particular interest to site engineers.

3.1.4.1 Block volume

Block size, which is determined from the joint spacing, joint orientation, number of joint sets and joint persistence, is an extremely important indicator of rock mass quality. The block volume can be calculated from

$$V_b = \frac{s_1 s_2 s_3}{\sin\gamma_1 \sin\gamma_2 \sin\gamma_3 \sqrt[3]{p_1 p_2 p_3}} \tag{5}$$

where s_i, γ_i and p_i are the joint spacing, the angle between joint sets, and joint persistence factor, respectively. If the joints are not persistent, *i.e.*, with rock bridges, the rock mass strength is higher and the global rock stability is enhanced. This effect can be considered using the concept of equivalent block volume as suggested in Cai *et al.* (2004). The consideration of joint persistency has been verified using numerical simulation by UDEC and 3DEC (Kim *et al.*, 2007). For persistent joint sets, $p_i = 1$. Blocks defined by three joint sets are shown in Figure 2.

Random joints may affect the shape and size of the block. Statistically, joint spacing follows a negative exponential distribution. For a rhombohedral block, the block volume is usually larger than that of cubic blocks with the same joint spacings. However, compared with the variation in joint spacing, the effect of the intersection angle between joint sets is relatively small. Hence, for practical purpose, for a rock mass containing persistent joint sets, the block volume can be approximated as

$$V_b = s_1 s_2 s_3 \tag{6}$$

Traditional methods for obtaining discontinuity data (joint sets, orientation, spacing, length, etc.) in the field include core/borehole logging, scanline survey, and cell mapping. Core/borehole logging alone cannot provide joint length information so that face mapping is needed to compensate. Scanline surveys, which are time consuming, provide detailed information on the individual joint in each set that can be used in probabilistic design, whereas cell mapping, which are easier and more efficient, only provides average information about each joint set. Decisions have to be made to select the most appropriate method to obtain the required information for block volume and joint surface condition factor (see Section 3.1.4.2) determination.

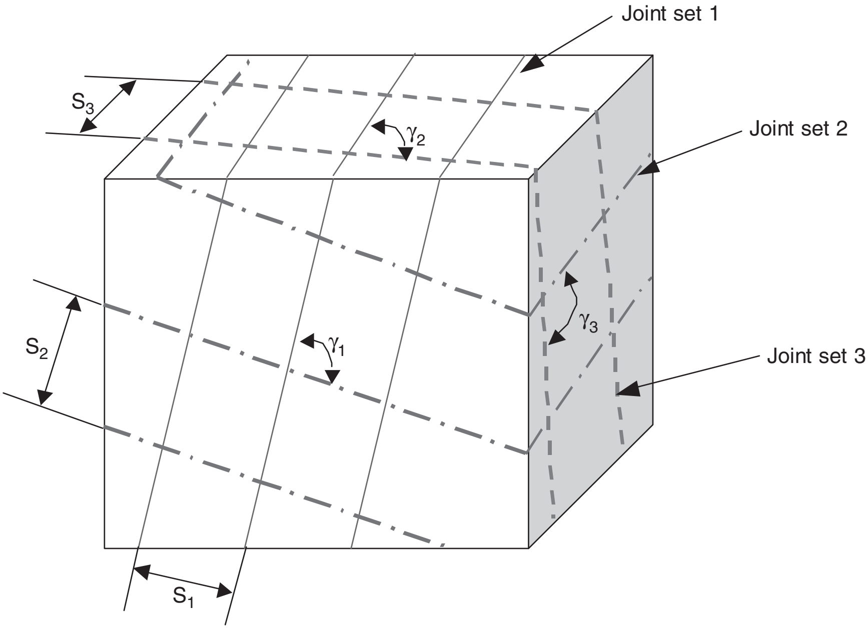

Figure 2 Block delimited by three joint sets.

3.1.4.2 Joint condition factor

In the GSI system, the joint surface condition is defined by the roughness, weathering, and infilling condition (Hoek *et al.,* 1995; Cai *et al.,* 2004). The combination of these factors defines the strength of a joint or block surface. The joint condition factor, J_c, used to quantify the joint surface condition, is defined as

$$J_C = \frac{J_W \cdot J_S}{J_A} \tag{7}$$

where J_W and J_S are the large-scale waviness (in meters from 1 to 10 m) and small-scale smoothness (in centimeters from 1 to 20 cm) and J_A is the joint alteration factor. The ratings for J_W, J_S, and J_A are listed in Table 3, Table 4, and Table 5, respectively.

3.1.4.3 Peak GSI value and strength parameters

The quantified GSI chart is presented in Figure 3. The descriptive block size is supplemented with the quantitative block volume (V_b) and the descriptive joint condition is supplemented with the quantitative joint condition factor (J_c). The influence of V_b and J_c on GSI was calibrated using published data (Cai *et al.*, 2004).

Once V_b and J_c are determined, users can use Figure 3 or the following equation (Cai & Kaiser, 2006b) to determine the peak GSI value.

Table 3 Terms to describe large-scale waviness (Palmstrøm, 1995).

Waviness terms	*Undulation*	*Rating for waviness J_W*
Interlocking (large-scale)		3
Stepped		2.5
Large undulation	> 3 %	2
Small to moderate undulation	0.3 – 3 %	1.5
Planar	< 0.3 %	1

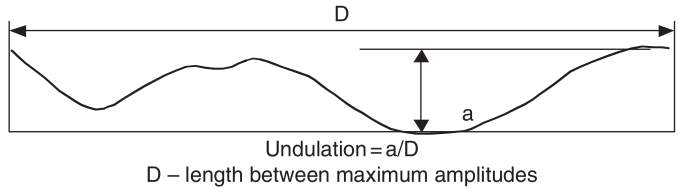

Table 4 Terms to describe small-scale smoothness (Palmstrøm, 1995).

Smoothness terms	*Description*	*Rating for J_S*
Very rough	Near vertical steps and ridges occur with interlocking effect on the joint surface	3
Rough	Some ridge and side-angle are evident; asperities are clearly visible; discontinuity surface feels very abrasive (rougher than sandpaper grade 30)	2
Slightly rough	Asperities on the discontinuity surfaces are distinguishable and can be felt (like sandpaper grade 30 – 300)	1.5
Smooth	Surface appear smooth and feels so to the touch (smoother than sandpaper grade 300)	1
Polished	Visual evidence of polishing exists. This is often seen in coating of chlorite and specially talc	0.75
Slickensided	Polished and striated surface that results from sliding along a fault surface or other movement surface	0.6 – 1.5

Table 5 Rating for the joint alteration factor J_A (Barton *et al.,* 1974; Palmstrøm, 1995).

	Term	*Description*	*JA*
Rock wall contact	**Clear joints** Healed or "welded' joints (unweathered)	Softening, impermeable filling (quartz, epidote etc.)	0.75
	Fresh rock walls (unweathered)	No coating or filling on joint surface, except for staining	1
	Alteration of joint wall: slightly to moderately weathered	The joint surface exhibits one class higher alteration than the rock	2
	Alteration of joint wall: highly weathered	The joint surface exhibits two classes higher alteration than the rock	4
	Coating or thin filling- Sand, silt, calcite etc.	Coating of frictional material without clay	3
	– Clay, chlorite, talc etc.	Coating of softening and cohesive minerals	4
Filled joints with partial or no contact between the rock wall surfaces	– Sand, silt, calcite etc.	Filling of frictional material without clay	4
	– Compacted clay materials	"Hard" filling of softening and cohesive materials	6
	– Soft clay materials	Medium to low over-consolidated of filling	8
	– Swelling clay materials	Filling material exhibits swelling properties	8 – 12

$$GSI(V_b, J_c) = \frac{26.5 + 8.79 \ln J_c + 0.9 \ln V_b}{1 + 0.0151 \ln J_c - 0.0253 \ln V_b} \tag{8}$$

where J_c is a dimensionless factor, and V_b is in cm^3. With GSI directly expressed as a function of V_b and J_c, the Hoek-Brown strength parameters (m_b, s, a) can also be directly expressed as a function of V_b and J_c. This convenience can facilitate the use of

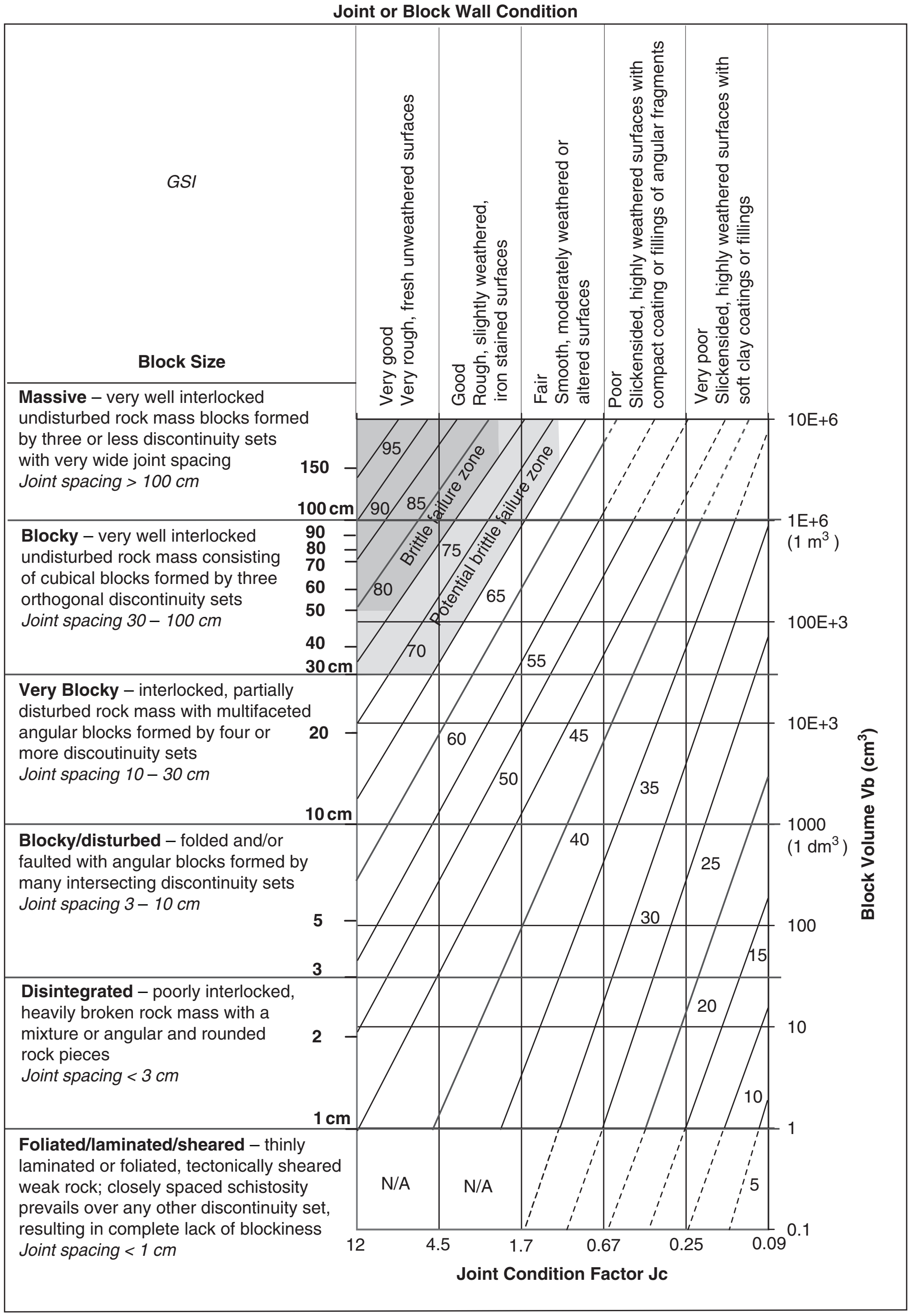

Figure 3 GSI chart (reproduced from (Cai *et al.*, 2004)).

probabilistic design approach to tunnel and cavern design using the GSI system (Cai & Kaiser, 2006a; Cai, 2011).

3.2 Residual strength parameters

3.2.1 Generalized Hoek-Brown failure criterion for residual strength

It is observed that a rock mass in its residual state represents one particular kind of rock mass in the spectrum in the GSI chart. The rock mass spectrum is defined by the combination of the block volume spectrum and the joint surface condition factor spectrum. The generalized Hoek-Brown failure criterion for the residual strength of jointed rock masses can be written as

$$\sigma_1 = \sigma_3 + \sigma_c \left(m_r \frac{\sigma_3}{\sigma_c} + s_r \right)^{a_r} \tag{9}$$

where m_r, s_r, a_r are the residual Hoek-Brown constants for the rock mass. As for the intact rock properties, fracturing and shearing do not weaken the intact rocks so that the mechanical parameters (σ_c and m_i) should be unchanged. Cai *et al.* (2007) considered that constants m_r, s_r, and a_r can be determined from a residual GSI_r value using the same equations for peak strength parameters. Because the rock masses are in a damaged, residual state, $D = 0$ is used for the residual strength parameter calculation. According to the logic of the original GSI system, the strength of a rock mass is controlled by its block size and joint surface condition. The same concept is valid for fractured rock masses at their residual strength state. In other words, the residual GSI_r is a function of residual joint surface condition factor J_c^r and residual block volume V_b^r (Cai *et al.*, 2007).

3.2.2 Residual GSI value and strength parameters

Once the residual block volume and joint surface condition factor are obtained, one can refer to the GSI chart or use the following equation to obtain the residual GSI value

$$GSI_r(V_b^r, J_c^r) = \frac{26.5 + 8.79 \ln J_c^r + 0.9 \ln V_b^r}{1 + 0.0151 \ln J_c^r - 0.0253 \ln V_b^r} \tag{10}$$

where J_c^r is a dimensionless factor, and V_b^r is in cm^3.

If a rock experiences post-peak deformation with sufficient straining, the rock in the broken zone is fractured and consequently turned into a "poor" and eventually "very poor" rock. For the residual block volume, it is observed that the post-peak block volumes are small because the rock mass has experienced tensile and shear fracturing with sufficient straining. After the peak load and with sufficient straining, the rock mass becomes less interlocked, and is heavily broken with a mixture of angular and partly-rounded rock pieces. Detailed examination of the rock mass damage state before and after the in-situ block shear tests at some underground cavern sites revealed that in areas that were not covered by concrete, the failed rock mass blocks were 1 to 5 cm in size. The rock mass was disintegrated along a shear zone in these tests. Hence, the residual block volumes can be considered independent of the original (peak) block volumes for most strain-softening rock masses. The fractured residual rock mass will have more or less the same residual block volume in the shear band for intact rocks, moderately jointed and highly jointed rock masses. As an estimate, Cai *et al.* (2007) recommended that if the peak block volume V_b is greater than 10 cm^3, then, the residual block volume V_b^r in the disintegrated category can be taken to be 10 cm^3. If V_b is smaller than 10 cm^3, then, no reduction to the residual block volume is recommended, *i.e.*, $V_b^r = V_b$.

The major factor that alters the joint surface condition in the post-peak region is the reduction of joint surface roughness. Using the concept of ultimate mobilized joint roughness suggested by Barton *et al.* (1985), the large-scale waviness and the small-scale smoothness of joints can be calculated by reducing its peak value by half to calculate the residual *GSI* value. The residual joint surface condition factor J_c^r can be calculated from (Cai *et al.,* 2007)

$$J_c^r = \frac{J_W^r \cdot J_S^r}{J_A^r} \tag{11}$$

where J_W^r, J_S^r, and J_A^r are residual values for large-scale waviness, small-scale smoothness, and joint alteration factor, respectively. The residual values are obtained based on the corresponding peak values assessed from field mapping. The reduction of J_W^r and J_S^r, from their peak values J_W and J_S, are based on the concept of mobilized joint roughness, and the equations are given as

$$\text{If } \frac{J_W}{2} < 1,\ J_W^r = 1;\quad \text{Else } J_W^r = \frac{J_W}{2} \tag{12}$$

$$\text{If } \frac{J_S}{2} < 0.75,\ J_S^r = 0.75;\quad \text{Else } J_S^r = \frac{J_S}{2} \tag{13}$$

In a short period, joint alteration is unlikely to occur so that the joint alteration factor J_A can be considered as unchanged in most circumstances.

3.3 Discussion on the use of the generalized Hoek-Brown failure criterion

The generalized Hoek-Brown failure criterion is only applicable to intact rock or to heavily jointed rock masses that can be roughly considered as homogenous and isotropic. The criterion should not be applied to highly schistose rocks such as slates or to rock masses in which the properties are controlled by a single set of discontinuities such as bedding planes (Hoek *et al.,* 1995). The criterion works well for rock masses at low confinement conditions and it should not be used for defining rock mass strength at very high confinement conditions.

Because of the inherent uncertainty of the intact rock properties and jointing in the rock mass, any estimate of rock mass strength parameters from using the Hoek-Brown failure criterion should not be considered as final. The approach is particularly useful in the preliminary design stage where only limited ranges of site characterization and test data are available. As the project progresses, field monitoring should be conducted to verify previously obtained approximate estimates of rock mass strength parameters. This is a process important for proper use of not only the Hoek-Brown failure criterion but also other failure criteria.

Pelli *et al.* (1991) found that the parameters obtained from Equations 2 and 3 did not predict the observed failure locations and extent near a tunnel in a cemented sand or siltstone. They found that lower m_b and higher s values were required to match predictions with observations. Further analyses of underground excavations in brittle rocks eventually lead to the development of brittle Hoek-Brown parameters (Martin *et al.,* 1999; Kaiser *et al.,* 2000; Diederichs, 2007) for massive to moderately fractured rock masses with tight interlock that fail by spalling or slabbing rather than by shear failure. Accordingly, Equations 2 and 3 are clearly not applicable for GSI > 75 in massive to moderately or discontinuously jointed hard rocks. The zone of anticipated brittle failure conditions is highlighted in Figure 3 by the hatched near the upper left corner.

The Hoek–Brown failure criterion was initially derived based on triaxial test data of intact rocks. Many data in the high confinement range were included and hence the criterion assumed a shear failure mechanism by default. The generalization to jointed rock mass also inherited this assumption of shear failure mechanism. Hence, care must be given when using the criterion outside the range of applicability of the assumptions and data on which it was based, such as the modeling of brittle failure of hard rocks in low confinement conditions. Brittle failure of hard massive rocks is governed by a process of gradual cohesion loss and friction mobilization (Martin, 1997; Kaiser *et al.,* 2000; Hajiabdolmajid *et al.,* 2002). The fundamental mechanism of this is tensile crack (Griffith crack) initiation, propagation, and coalescence in low to zero confinement environments. Using conventional strength parameters derived from Hoek–Brown criterion to model brittle rock failure was found less useful and less successful because the failure zones around excavations could not be predicted satisfactorily. Specific brittle failure parameters, including both peak and residual ones, are required to model brittle failure of massive rocks adequately (Cai & Kaiser, 2014).

The generalized Hoek–Brown criterion may not be applied to weak rocks with, for σ_c < 15 MPa, because it has been found that, at these low strengths, the index, *a*, can be greater than the maximum value of about 0.65 given by Equation 4 and can approach one (Brown, 2008).

4 ESTIMATION DEFORMATION MODULUS

The deformation modulus of the jointed rock mass is required when carrying out numerical analysis in design. Traditional method to determine the deformation modulus is through in-situ plate loading tests or using back analysis based on measured displacements of excavations. As discussed in Section 2.2, there are many empirical equations to correlate rock mass deformation modulus with some rock mass classification indexes. One important thing to remember is the applicable boundary conditions for each individual equation (as show in Table 1 of the "Note" column). When the boundary is crossed, meaningless deformation modulus can be obtained.

Blasting tends to loosen rock mass and reduce its deformation modulus. Hence, including the factor *D* in the empirical equation allows us to consider the effects of blast damage and stress relaxation. The deformation modulus is related to the GSI value as (Hoek *et al.,* 2002)

$$E = \left(1 - \frac{D}{2}\right)\sqrt{\frac{\sigma_c}{100}}10^{\left(\frac{GSI-10}{40}\right)},\ \text{(GPa)} \quad \text{for } \sigma_c < 100\text{MPa} \tag{14}$$

The inclusion of σ_c in Equation 14 shows indirectly the influence of the modulus of the intact rock (E_i) on the deformation modulus of the rock mass, because there is a good correlation between E_i and σ_c (Deere, 1968). A more recent update on the deformation of modulus of jointed rock mass is (Hoek & Diederichs, 2006)

$$E = E_i\left(\frac{1 - D/2}{1 + e^{((75+25D-GSI)/11)}}\right) \tag{15}$$

Equation 15 considers the influence of intact rock modulus directly and avoids unrealistically high values of rock mass deformation moduli when the GSI value is high. In general, the rock mass deformation moduli can be highly anisotropic, and are also confining stress dependent (Barton, 2002; Cai & Kaiser, 2002). Those features need to be properly addressed in order to correctly predict deformation distribution in the rock mass around excavations. Unfortunately, there exist no simple equations that relate the deformation modulus to confining stress.

5 DILATION ANGLE

When a rock or a rock mass fails, its volume increases and this phenomenon is known as dilation. The excavation-induced rock failure and displacement near an underground opening boundary is closely associated with rock mass dilation. A better understanding of rock mass dilation around the excavation helps us to predict or anticipate displacements and failure extent and shape, and subsequently assist the design of proper ground support systems.

In addition to rock mass strength (both peak and residual) and deformation modulus, most numerical tools (*e.g.*, Phase2, FLAC) require another important input parameter – dilation angle. The dilation angle is not only a suitable parameter for the description of soil dilation, but also appears to be useful for rocks to describe rock dilation.

However, in rock engineering, when the dilation angle is taken into consideration, especially for numerical modeling studies, the approach employed by most researchers is often simplistic; it is generally assumed as either one of the two constants – zero in a non-associated flow rule and the same as the friction angle in an associated flow rule. In the most popular failure criteria, such as linear Mohr-Coulomb failure criterion and non-linear Hoek-Brown failure criterion, the rock dilation is assumed to remain as a constant when the rock mass is deformed.

Hoek and Brown (1997), based on wide engineering experience, suggest the use of constant dilation angle values that are dependent on rock mass quality. For very good rock, they recommended that the dilation angle is about 1/4 of the friction angle; for the average quality rock, the value suggested is 1/8, and poor rock seems to have a negligible dilation angle.

In reality, a constant dilation angle is an approximation that is clearly not physically sound. This constant dilation assumption is made largely because little is known about how the dilation of a rock changes past peak load. Some researchers (Detournay, 1986;

Alejano & Alonso, 2005) illustrate that it may be unrealistic and misleading to use a constant dilation angle. They also point out that dilation angle should be a function of plastic parameters and confining stress.

A few dilation models have been proposed for rocks, considering the influence of plastic strain (Detournay, 1986) and confining stress (Alejano & Alonso, 2005). A more recent empirical mobilized dilation angle model considers the influence of both confining stress and plastic shear strain (Cai & Zhao, 2010; Zhao & Cai, 2010a,b). The empirical dilation angle model was derived based on published data acquired from modified triaxial compression tests with volumetric strain measurement. Based on the model response and in combination with the grain size description and the uniaxial compressive strength of rocks, the model parameters for four rock types (coarse-grained hard rock, medium-grained hard rock, fine-medium-grained soft rock, and fine-grained soft rock) are suggested. New test data (Arzua & Alejano, 2013) support the validity of the mobilized dilation angle model.

For jointed rock masses, it is suggested to estimate the peak dilation angle from the peak friction angle of rock mass determined by the GSI system (Cai & Zhao, 2010; Zhao & Cai, 2010b). It is also assumed that the dilation behavior of jointed rock masses follow similar trend as observed for in tact rocks so that the empirical relations established for intact rocks can be applied to jointed rock masses. In this fashion, plastic strain and confinement dependent dilation angles can be defined for jointed rock masses. One example is presented in Figure 4. The dilation angle is zero when there is no plastic deformation; it increases rapidly and reaches a peak value at a small plastic deformation when the confinement is low. When confining stress increases, a general trend is that the peak dilation angles decrease and the locations of peak dilation angle gradually shift toward right with more plastic shear straining. Confinement drastically reduces rock dilation. For example, a 5 MPa confinement can reduce the peak dilation angle of the intact rock from 53° at zero confinement to about 12°. As plastic deformation continues, the dilation angles decrease gradually until an asymptotic low value is reached. This makes sense as dilation rate will reduce as the rocks deform. At zero confinement, the peak dilation angle of the intact rock reduces from 53° to 38° for a jointed sandstone with GSI = 50.

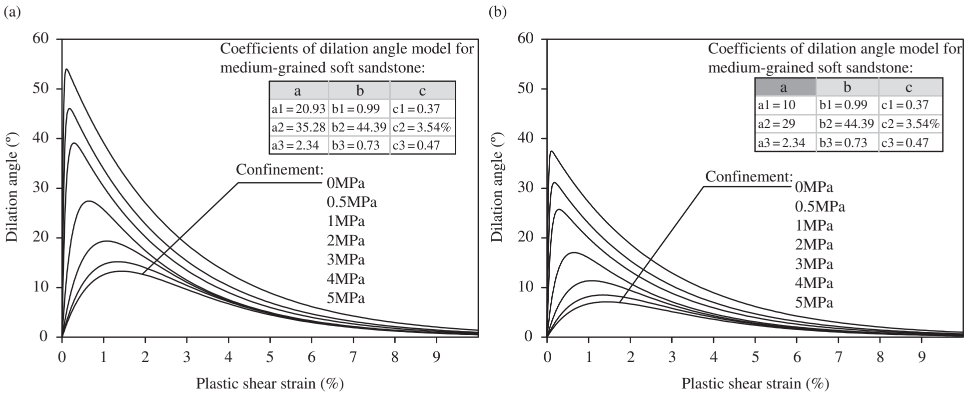

Figure 4 (a) Dilation angle variation for intact rock (medium-grained soft sandstone); (b) Dilation angle variation for a jointed sandstone with GSI = 50.

The mobilized dilation angle model can be easily implemented into some numerical tools such as FLAC and FLAC3D. Displacement distributions obtained from using the dilation angle model are more reasonable, when compared with the general trend measured underground. The generation of large deformations near the excavation boundary is attributed to the existence of low to zero confinements. The displacement decreases rapidly as confinement increases. Rock dilation behavior near the excavation boundary such as this can only be properly simulated when a dilation angle model, which considers the influence of both plastic shear strain and confinement, is used.

6 APPLICATION EXAMPLE

One of the long-standing challenges in analyzing rock mass strength and deformation data is attributed to the fact that these values are quite variable. The intact rock strength, joint spacing, and joint surface condition vary even within the same rock type zone. In rock engineering practice, geological and geotechnical data, because of the huge cost involved in their acquisition, are often incomplete and hence contain uncertainties. Uncertainties are inherent and unavoidable in the rock mass classification/characterization process. Common sources of uncertainties in rock engineering include the spatial and temporal variability of the rock mass properties; random and systematic errors in data mapping, logging, testing, and monitoring; analytical and numerical model simplification; human omissions and errors. In engineering design, the appropriate approach is to cope with the uncertainties, to assess and manage the risk associated with them, *i.e.*, to incorporate uncertainties into the design and decision-making process.

One advantage of the quantitative GSI system approach is that the variability of inherent parameters can be explicitly considered in the calculation process (Cai & Kaiser, 2006a). The closed-form solution to obtain GSI values from dependent variables such as joint spacing, orientation, persistence, surface condition factor, etc., makes it suitable for probabilistic analysis using the Monte Carlo method. The variability of strength and deformation parameters can be implemented in the design tools to calculate the variability of stress and deformations as well as anticipated loads in rockbolts and anchors.

To apply the GSI system for rock mass characterization, two groups of parameters need to be determined. One is the intact rock parameters, which includes σ_c and m_i. Another is the joint parameters, which is further divided into the joint geometry and strength subgroups. All these parameters can be considered as random variables. In general, a normal distribution with the mean and the coefficient of variation (COV) can be used to describe the probability distribution of σ_c and m_i.

Priest and Hudson (1976) stated that statistically, joint spacing follows a negative exponential distribution. However, some researchers consider that the joint spacing distribution is logarithmic. If the interaction of jointing corresponds to the multiplicatory process, lognormal distribution may result (Dershowitz & Einstein, 1988). The type of distribution seems to be affected by the minimum bin size used in the histogram analysis of joint spacing. In the example shown here, lognormal distribution is applied for joint spacing.

Joint orientation affects both the block shape and size, and it is usually defined by joint dip and dip direction. Joint orientations are stochastic but quite often cluster in preferred orientations to form joint sets. The joint orientation variability is thus governed by the degree of clustering within each set. The Fisher distribution is often used to describe the joint orientation distribution.

Joint sizes and trace lengths vary even a wide range and are difficult to be determined accurately. Several distributions, such as exponential, lognormal, hyperbolic, Gamma-1 distributions, have been proposed to describe the joint trace lengths. The variability in joint size includes the inherent natural randomness of this property and our limited ability to measure or model this property, rendering it one of the most difficult parameters in joint system modeling. Priest and Hudson (1981) used the negative exponential distribution to describe the joint lengths. Depending on the problem scale and bin size used, both negative exponential distribution and lognormal distribution are appropriate to describe the joint length distribution.

The joint surface condition factor is a measure of the joint strength against shearing. In practice, when the small-scale joint smoothness is, on average, "rough," there are possibilities that some portions of the joint are "very rough" while other portions are "slightly rough." This uncertainty can result from both spatial variability of the joint surface condition and human discrepancy in field mapping. A decision therefore has to be made about the rating range and the distribution type. For simplicity, the normal distribution can be used to represent the joint roughness and alteration variability. When the mean values are near the extreme values in the rating, a truncated normal distribution can be used.

In the following illustration example, we consider the rock mass classification for a rock mass at a large-scale hydropower cavern site in Japan and assume that the joint spacing follows a lognormal distribution. Details about the cavern construction project can be found in Koyama *et al.* (1997). Three orthogonal joint sets exist and the average joint spacing for the three joint sets is 10, 25, and 50 cm and the standard deviations are 3, 7.5, and 15 cm, respectively. Using the Monte Carlo simulation technique available in @RISK, the probability distribution function (PDF) of the block volume for the rock mass is calculated using 5000 iterations and the result is presented in Figure 5(a). It is seen that the block volume follows a lognormal distribution.

It was determined from field mapping that the average values for large-scale joint waviness J_w, small-scale smoothness J_s, and joint alteration J_A are 2, 2, and 1, respectively, and the coefficients of variation for all three factors were assumed to be 8%. Truncated normal distributions are assumed for J_w, J_s, and J_A. The truncation is based on the minimum and maximum ratings for each parameter. For example, J_w should not be less than 1 and not greater than 3. J_w is thus described by a normal distribution with a mean of 2 and standard deviation of 0.16, truncated at 1 and 3. J_c thus calculated also follows a normal distribution as shown in Figure 5(b).

Equation 9 is used to calculate the *GSI* distribution based on V_b and J_c, again using the Monte Carlo method. Although V_b follows a lognormal distribution, the calculated *GSI* values follow a normal distribution, as shown in Figure 12(c). The average *GSI* is 59.9 with a standard deviation of 2.1. The probability density distributions for the Hoek-Brown strength parameters m_b and s are presented in Figure 12(d & e), and it is found that the m_b values follow a normal distribution. Although the s values are best

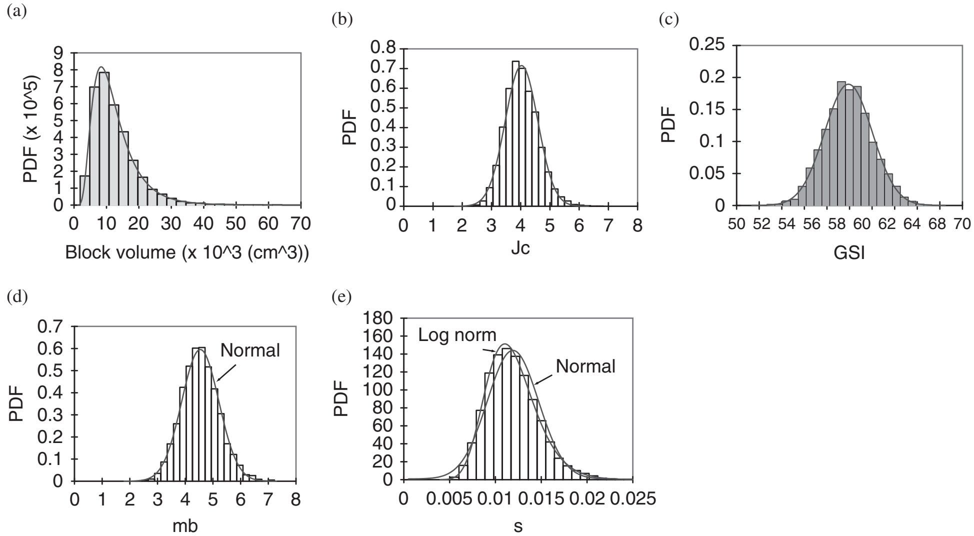

Figure 5 (a) Block volume Vb; (b) Jc; (c) *GSI* distributions; (d) m_b; (e) s simulated using @ RISK.

described by a lognormal distribution, it can also be approximated by a normal distribution as shown in the figure. It is seen from the results that the *GSI* value and hence the mechanical properties of the jointed rock masses exhibit variability. These properties are not just the average values, but have a distribution about the means, even under ideal conditions. The design will make more sense if these property distributions are properly considered.

Based on the variability information about the rock mass strength and deformability, stability analysis can be performed using the point estimate method (PEM) (Rosenblueth, 1981) in combination with a FEM analysis program, which considers the possible combinations of strength and deformation parameters as well as in-situ stress. PEM is an alternative to Monte Carlo simulation with models containing a limited number of uncertain inputs. In this method, the model is evaluated at a discrete set of points in the uncertain parameter space, with the mean and variance of model predictions computed using a weighted average of these functional evaluations.

As the output of the analysis, the probability distributions of yielding or loosening zones and total displacements in the roof and on the sidewalls of the cavern can be obtained. As an example, the probability density function of the yielding zone distribution around the cavern is presented in Figure 6, with the consideration of material variability alone. 15 m long pre-stressed (PS) anchors had been selected for cavern support. It is seen that the probability that the 15 m anchor may be shorter than the yielding zone depth on the right sidewall is 0.0077 %, and the probability that the anchor's 3 m anchorage length may fall in the yielding zone is 1.3 %. It is obvious that cost saving in terms of reducing the support quantities is achievable if a certain level of risk is acceptable. The simulation results allow us to better understand how uncertainty arises and how the rock support system design decision may be affected by it.

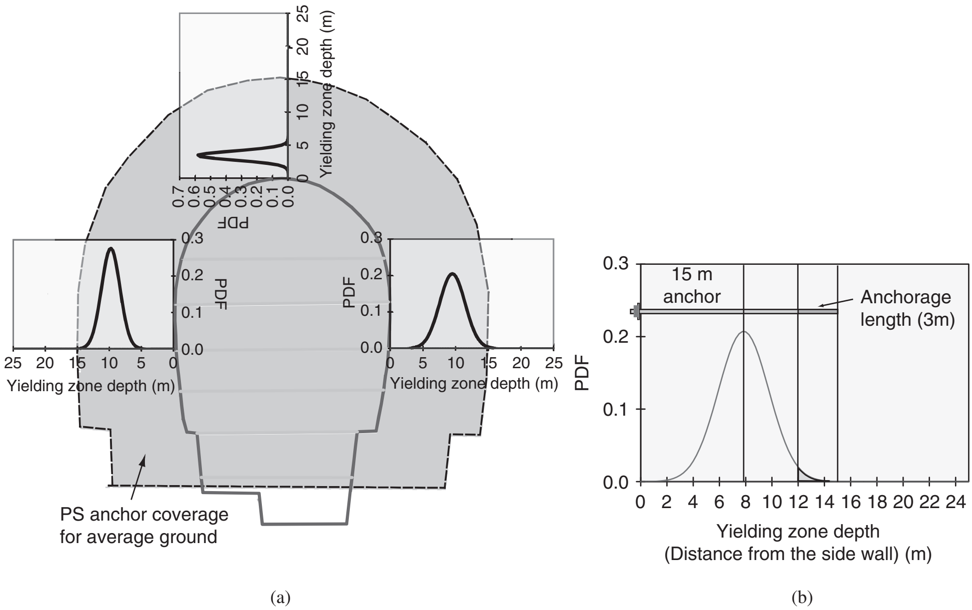

Figure 6 (a) Probability distributions of the yielding zone depths in the roof and on the sidewalls; (b) enlarged figure of probability distribution on the right sidewall. The cavern dimensions are: width 34 m, height 54 m, located 500 m underground.

7 CONCLUSION

Different from other rock mass classification systems, the GSI system is directly linked to engineering parameters such as Mohr-Coulomb or Hoek-Brown strength parameters or rock mass deformation modulus. The original GSI system, which is applied mainly for the estimation of the peak strength, is based on a descriptive approach, rendering the system somewhat subjective and difficult to use for inexperienced personnel. To assist the use of the GSI system, a supplementary quantified approach for the GSI system, which incorporates quantitative measures of block volume and joint surface condition factor, can be used. The block volume can be calculated, in most cases, from joint spacings of three dominant joint sets. The joint condition factor is obtained by rating joint roughness depending on the large-scale waviness, small-scale smoothness of joints, and joint alteration depending on the weathering and infillings in joints.

The concept of residual block volume V_b^r and residual joint surface condition factor J_c^r was used to extend the GSI system for the estimation of rock mass's residual strength. The residual strength parameters can be calculated using the same form of the generalized Hoek-Brown strength criterion by assuming that the intact rock properties such as σ_c and m_i remain unchanged as the rock mass changes from its peak state to its residual state.

The quantitative approach for peak and residual strength estimation extends the GSI system and adds quantitative means to determine the complete set of rock mass strength properties needed for design. In addition, the approach is built on the linkage between descriptive geological terms and measurable field parameters such as joint spacing and joint roughness, which are random variables. Because of its quantitative nature, it allows the evaluation of both the means and variances of strength and deformation parameters, using the Monte Carlo or point estimate method.

When using the generalized Hoek-Brown strength criterion in design, we should pay not only more attention to the determination of GSI values more objectively, but also sufficient attentions to the determination of other parameters such as σ_c, m_i, D, and dilation angle. It is suggested that at least simple uniaxial compression tests should be conducted to obtain σ_c and m_i values more accurately. Test specimens should be strain-gauged to define the crack initiation stress level σ_{ci} and then the m_i value can be estimated using $m_i = 8\ \sigma_c/\sigma_{ci}$.

Although this chapter provides a contemporary method for obtaining rock mass mechanical parameters needed in engineering design, its successful application relies heavily on the professional judgment, as is typically the case in rock mechanics and rock engineering.

ACKNOWLEDGMENTS

The author wishes to thank Tokyo Electric Power Services Co. Ltd (TEPSCO) and Tokyo Electric Power Company (TEPCO) for their financial support to this study, and the contributions and constructive comments provided by Dr. P. Kaiser of Laurentian University (Emeritus Professor), Dr. E. Hoek of Evert Hoek Consulting Engineer Inc., Dr. D. McCreath of Laurentian University (Emeritus Professor), Mr. Y. Tasaka and Dr. H. Uno of TEPSCO, Mr. M. Minami of TEPCO, and Dr. X. Zhao of Beijing Research Institute of Uranium Geology.

REFERENCES

Alejano, L. R. & Alonso, E. (2005) Considerations of the dilatancy angle in rocks and rock masses. Int. J. Rock Mech. Min. Sci. 42(4), 481–507.

Alejano, L. R., Rodriguez-Dono, A., Alonso, E., & Fdez.-Manin, G. (2009) Ground reaction curves for tunnels excavated in different quality rock masses showing several types of post-failure behaviour. Tunnelling Underground Space Technol. 24(6), 689–705.

Amadei, B. (1988) Strength of a regularly jointed rock mass under biaxial and axisymmetric loading. Int. J. Rock Mech. Min. Sci. Geomech. Abstr. 25(1), 3–13.

Arzua, J., & Alejano, L. R. (2013) Dilation in granite during servo-controlled triaxial strength tests. Int. J. Rock Mech. Min. Sci. 61, 43–56.

Aydan, O. & Dalgiç, S. (1998) Prediction of deformation behavior of 3-lanes Bolu tunnels through squeezing rocks of North Anatolian fault zone (NAFZ). In: Proceedings of Regional Symposium on Sedimentary Rock Engineering, Taipei, 228–233.

Barton, N. (2002) Some new Q-value correlations to assist in site characterisation and tunnel design. Int. J. Rock Mech. Min. Sci. 39(2), 185–216.

Barton, N. R., Bandis, S. C. & Bakhtar, K. (1985) Strength, deformation and conductivity coupling of joints. Int. J. Rock Mech. Min. Sci. Geomech. Abstr. 22(3), 121–140.

Barton, N. R., Lien, R. & Lunde, J. (1974) Engineering classification of rock masses for the design of tunnel support. Rock Mech. 6(4), 189–239.

Barton, N. R., Loset, F., Lien, R. & Lunde, J. (1980) Application of the Q-system in design decisions concerning dimensions and appropriate support for underground installations. In: Int. Conf. Subsurface Space, Rockstore, Stockholm, 553–561.
Bhasin, R. & Grimstad, E. (1996) The use of stress-strength relationships in the assessment of tunnel stability. Tunnelling Underground Space Technol. 11(1), 93–98.
Bieniawski, Z. T. (1976) Rock mass classification in rock engineering. In: Proc. Symp. on Exploration for Rock Engineering, Balkema, Cape Town, 97–106.
Bieniawski, Z. T. (1978) Determining rock mass deformability – experience from case histories. Int. J. Rock Mech. Min. Sci. Geomech. Abstr. 15(5), 237–247.
Brown, E. T. (2008) Estimating the mechanical properties of rock masses. In: SHIRMS 2008, 3–21.
Cai, M. (2010) Practical estimates of tensile strength and Hoek-Brown strength parameter mi of brittle rocks. Rock Mech. Rock Eng. 43(2), 167–184.
Cai, M. (2011) Rock mass characterization and rock property variability considerations for tunnel and cavern design. Rock Mech. Rock Eng. 44(4), 379–399.
Cai, M. & Horii, H. (1992) A constitutive model of highly jointed rock masses. Mech. Mater. 13, 217–246.
Cai, M. & Kaiser, P. K. (2002) Dependency of wave propagation velocity on rock mass quality and confinement. In: NARMS 2002, University of Toronto Press, 615–622.
Cai, M. & Kaiser, P. K. (2006a) Rock mass characterization and rock mass property variability considerations for tunnel and cavern design. In: Proc. 4th Asian Rock Mech. Symp. (ARMS 4), World Scientific, Singapore, Paper 144.
Cai, M. & Kaiser, P. K. (2006b) Visualization of rock mass classification systems. Geotech. Geol. Eng. 24(4), 1089–1102.
Cai, M. & Kaiser, P. K. (2014) In-situ rock spalling strength near excavation boundaries. Rock Mech. Rock Eng. 47(2), 659–675.
Cai, M., Kaiser, P. K., Tasaka, Y. & Minami, M. (2007) Determination of residual strength parameters of jointed rock masses using the GSI system. Int. J. Rock Mech. Min. Sci. 44(2), 247–265.
Cai, M., Kaiser, P. K., Uno, H., Tasaka, Y. & Minami, M. (2004) Estimation of rock mass strength and deformation modulus of jointed hard rock masses using the GSI system. Int. J. Rock Mech. Min. Sci. 41(1), 3–19.
Cai, M., Morioka, H., Kaiser, P. K., Tasaka, Y., Minami, M. & Maejima, T. (2007) Back analysis of rock mass strength parameters using AE monitoring data. Int. J. Rock Mech. Min. Sci. 44(4), 538–549.
Cai, M. & Zhao, X. G. (2010) A confinement and deformation dependent dilation angle model for rocks. In: Proc. 44th US Rock Mech. Symp. and 5th U.S.-Canada Rock Mech. Symp., Paper 459, Salt Lake City, UT.
Cividini, A., Gioda, G. & Jurina, L. (1981) Some aspects of 'characterization' problems in geomechanics. Int. J. Rock Mech. Min. Sci. Geomech. Abstr. 18, 487–503.
Coon, R. F. & Merritt, A. H. (1970) Predicting in situ modulus of deformation using rock quality indices. In: Determination of the In Situ Modulus of Deformation of Rock, ASTM STP 477, 154–173.
Deere, D. U. (1968). "Geological consideration." Rock Mechanics in Engineering Practice, K. G. Stagg and O. C. Zienkiewicz, eds., John Wiley & Sons, New York, 1–20.
Deere, D. U., Hendron, A. J., Patton, F. D. & Cording, E. J. (1967) Design of surface and near surface construction in rock. In: Failure and breakage in rock, 237–302.
Dershowitz, W. S. & Einstein, H. H. (1988) Characterizing rock joint geometry with joint system models. Rock Mech. Rock Eng. 21(1), 21–51.
Dershowitz, W. S., Lee, G., Geier, J., Hitchcock, S. & la Pointe, P. (1993). *Support of underground excavations in hard rock*. Golder Associates, Seattle.

Detournay, E. (1986) Elastoplastic model of a deep tunnel for a rock with variable dilatancy. Rock Mech. Rock Eng. 19(2), 99–108.

Diederichs, M. S. (2007) The 2003 Canadian Geotechnical Colloquium: Mechanistic interpretation and practical application of damage and spalling prediction criteria for deep tunnelling. Can. Geotech. J. 44(9), 1082–1116.

Fischer, L., Amann, F., Moore, J. R., & Huggel, C. (2010) Assessment of periglacial slope stability for the 1988 Tschierva rock avalanche (Piz Morteratsch, Switzerland). Eng. Geol. 116(1–2), 32–43.

Ghafoori, M., Lashkaripour, G. R. & Tarigh Azali, S. (2011) Investigation of the geological and geotechnical characteristics of Daroongar Dam, Northeast Iran. Geotech. Geol. Eng. 29(6), 961–975.

Gischig, V., Amann, F., Moore, J. R., Loew, S., Eisenbeiss, H., & Stempfhuber, W. (2011) Composite rock slope kinematics at the current Randa instability, Switzerland, based on remote sensing and numerical modeling. Eng. Geol. 118(1–2), 37–53.

Hajiabdolmajid, V., Kaiser, P. K. & Martin, C. D. (2002) Modelling brittle failure of rock. Int. J. Rock Mech. Min. Sci. 39(6), 731–741.

Hashemi, M., Moghaddas, S., & Ajalloeian, R. (2010) Application of rock mass characterization for determining the mechanical properties of rock mass: A comparative study. Rock Mech. Rock Eng. 43(3), 305–320.

Hoek, E. (1983) Strength of jointed rock masses. Geotechnique 33(3), 187–223.

Hoek, E. (2007) Practical Rock Engineering. Available online: www.rocscience.com, 342.

Hoek, E. and Brown, E. T. (1980) Underground excavations in rock. Institution of Mining and Metallurgy, London, 527.

Hoek, E. & Brown, E. T. (1988) The Hoek-Brown failure criterion – a 1988 update. In: Rock engineering for underground excavations, Proc. 15th Canadian Rock Mech. Symp., University of Toronto, Toronto, Toronto, Canada, 31–38.

Hoek, E. & Brown, E. T. (1997) Practical estimates of rock mass strength. Int. J. Rock Mech. Min. Sci. 34(8), 1165–1186.

Hoek, E., Carranza_Torres, C. & Corkum, B. (2002) Hoek-Brown failure criterion – 2002 edition. In: Proc. 5th North American Rock Mech. Symp., Toronto, Canada, 267–273.

Hoek, E., Carter, T. G. & Diederichs, M. S. (2013) Quantification of the geological strength index chart. In: 47th US Rock Mechanics/Geomechanics Symposium, San Francisco, CA, USA, ARMA 13–672.

Hoek, E. & Diederichs, M. S. (2006) Empirical estimation of rock mass modulus. Int. J. Rock Mech. Min. Sci. 43(2), 203–215.

Hoek, E., Kaiser, P. K. & Bawden, W. F. (1995) Support of underground excavations in hard rock. Taylor & Francis, New York, 215.

Hoek, E., Marinos, P. & Benissi, M. (1998) Applicability of the geological strength index (GSI) classification for very weak and sheared rock masses. The case of Athens Schist Formation. Bull. Eng. Geol. Env. 57, 151–160.

Hudson, J. A. & Harrison, J. P. (1997) Engineering rock mechanics – an introduction to the principles. Elsevier Science Ltd. UK, 444.

Itasca (2010) PFC3D-Particle Flow Code. Itasca Consulting Group Inc., 4.0.

Jade, S. & Sitharam, T. G. (2003) Characterization of strength and deformation of jointed rock mass based on statistical analysis. Int. J. Geomech. ASCE. 3, 43–54.

Kaiser, P. K., Diederichs, M. S., Martin, C. D., Sharp, J. & Steiner, W. (2000) Underground works in hard rock tunnelling and mining. In: Keynote lecture at GeoEng2000, Technomic Publishing Co., Melbourne, Australia, 841–926.

Kalamaras, G. S. & Bieniawski, Z. T. (1993) A rock mass strength concept for coal seams. In: Proceedings of 12th Conf. Ground Control in Mining, Morgantown, 274–283.

Kendorski, F. S., Cummings, R. A., Bieniawski, Z. T. & Skinner, E. H. (1983) Rock mass classification for block caving mine drift support. In: Proc. 5th ISRM, Melbourne, Australia, 51–63.
Kim, B. H., Cai, M., Kaiser, P. K. & Yang, H. S. (2007) Estimation of block sizes for rock masses with non-persistent joints. Rock Mech. Rock Eng. 40(2), 169–192.
Koyama, T., Nanbu, S. & Komatsuzaki, Y. (1997) Large-scale cavern at a depth of 500 m. Tunnel underground 28(1), 37–45. (in Japanese).
Laubscher, D. H. (1984) Design aspects and effectiveness of support system in different mining conditions. Trans. Inst. Min. Met. 93, A70–81.
Laubscher, D. H. (1990) A geomechanics classification system for the rating of rock mass in mine design. J. South Afr. Inst. Min. Metall. 90(10), 257–273.
Martin, C. D. (1993) The strength of massive Lac du Bonnet granite around underground opening. Ph.D. thesis, University of Manitoba, 278.
Martin, C. D. (1997) Seventeenth Canadian Geotechnical Colloquium: The effect of cohesion loss and stress path on brittle rock strength. Can. Geotech. J. 34(5), 698–725.
Martin, C. D., Kaiser, P. K. & McCreath, D. R. (1999) Hoek-Brown parameters for predicting the depth of brittle failure around tunnels. Can. Geotech. J. 36(1), 136–151.
Mas Ivars, D., Pierce, M. E., Darcel, C., Reyes-Montes, J., Potyondy, D., Young, R. P. & Cundall, P. (2011) The synthetic rock mass approach for jointed rock mass modelling. Int. J. Rock Mech. Min. Sci. 48(2), 219–244.
Nicholson, G. A. & Bieniawski, Z. T. (1990) A nonlinear deformation modulus based on rock mass classification. Int. J. Min. Geol. Eng. 8, 181–202.
Oda, M. (1983) A method for evaluating the effect of crack geometry on the mechanical behavior of cracked rock masses. Mech. Mater. 2, 163–171.
Palmstrøm, A. (1995) RMi – a rock mass characterization system for rock engineering purposes. Ph. D. thesis, University of Oslo, Norway, 400.
Palmstrøm, A. (1996a) Characterizing rock masses by the RMi for use in practical rock engineering, Part 1: The development of the rock mass index (RMi). Tunnelling Underground Space Technol. 11(2), 175–188.
Palmstrøm, A. (1996b) Characterizing rock masses by the RMi for use in practical rock engineering, Part 2: Some practical applications of the rock mass index (RMi). Tunnelling Underground Space Technol. 11(3), 287–303.
Pelli, F., Kaiser, P. K. & Morgenstern, N. R. (1991) An interpretation of ground movements recorded during construction of the Donkin-Morien tunnel. Can. Geotech. J. 28(2), 239–254.
Pierce, M., Cundall, P., Potyondy, D. & Mas Ivars, D. (2007) A synthetic rock mass model for jointed rock. In: Proc. 1st Canada-U.S. Rock Mechanics Symposium, Taylor & Francis, Vancouver, 341–349.
Potvin, Y. (1988) Empirical open stope design in Canada. Ph.D. thesis, Dept. Mining and Mineral Processing, University of British Columbia.
Priest, S. D. & Hudson, J. A. (1976) Discontinuity spacings in rock. Int. J. Rock Mech. Min. Sci. Geomech. Abstr. 13(5), 135–148.
Priest, S. D. & Hudson, J. A. (1981) Estimation of discontinuity spacing and trace length using scanline surveys. Int. J. Rock Mech. Min. Sci. Geomech. Abstr. 18(3), 183–197.
Ramamurthy, T. (1994) Strength predictions for jointed rocks in confined and unconfined states. Int. J. Rock Mech. Min. Sci. Geomech. Abstr. 31, 9–22.
Ramamurthy, T., Rao, G. V. & Rao, K. S. (1985) A strength criterion for rocks. In: Indian Geotech. Conf., Roorkee, 59–64.
Read, S., Richards, L. & Perrin, N. (1999) Applicability of the Hoek-Brown failure criterion to New Zealand greywacke rocks. In: 9th ISRM, 655–660.
Rockfield Software Ltd. (2003) ELFEN. 3.7.
Rosenblueth, E. (1981) Two-point estimates in probabilities. J. Appl. Math. Modell. 5(5), 329–335.

Russo, G. (2009) A new rational method for calculating the GSI. Tunnelling Underground Space Technol. 24(1), 103–111.

Sakurai, S. & Takeuchi, K. (1983) Back analysis of measured displacement of tunnels. Rock Mech. Rock Eng. 16, 173–180.

Serafim, J. L. & Pereira, J. P. (1983) Consideration of the geomechanical classification of Bieniawski. In: Proc. Int. Symp. on Engineering Geology and Underground Construction, Lisbon, 33–44.

Sheorey, P. R., Biswas, A. K. & Choubey, V. D. (1989) An empirical failure criterion for rocks and jointed rock masses. Eng. Geol. 26, 141–159.

Soleiman Dehkordi, M., Shahriar, K., Moarefvand, P., & Gharouninik, M. (2013) Application of the strain energy to estimate the rock load in squeezing ground condition of Eamzade Hashem tunnel in Iran. Arabian J. Geosci. 6(4), 1241–1248.

Sonmez, H., Gokceoglu, C. & Ulusay, R. (2004) Indirect determination of the modulus of deformation of rock masses based on the GSI system. Int. J. Rock Mech. Min. Sci. 41(5), 849–857.

Sonmez, H. & Ulusay, R. (1999) Modifications to the geological strength index (GSI) and their applicability to stability of slopes. Int. J. Rock Mech. Min. Sci. 36(6), 743–760.

Terzaghi, K. (1946) Rock defects and loads on tunnel supports. In: Rock Tunneling with Steel Supports, 17–99.

Wickham, G. E., Tiedemann, H. R. & Skinner, E. H. (1974) Ground support prediction model – RSR concept. In: Proc. 1st Rapid Excavation and Tunnelling Conference, Am. Inst. Min. Eng., 691–707.

Yudhbir, L. W., Lemanza, W. & Prinzl, F. (1983) An empirical failure criterion for rock masses. In: 5th ISRM, Balkema, B1–B8.

Zhang, L. (2010) Estimating the strength of jointed rock masses. Rock Mech. Rock Eng. 43(4), 391–402.

Zhang, L. & Einstein, H. H. (2004) Using RQD to estimate the deformation modulus of rock masses. Int. J. Rock Mech. Min. Sci. 41(4), 337–341.

Zhao, X. G. & Cai, M. (2010a) Influence of plastic strain and confinement dependent rock mass dilation on the failure and displacement near an excavation boundary. Int. J. Rock Mech. Min. Sci. 47(5), 723–738.

Zhao, X. G. & Cai, M. (2010b) A mobilized dilation angle model for rocks. Int. J. Rock Mech. Min. Sci. 47(3), 368–384.